Original Article
Food Science and Technology

ISSN 0101-2061 (Print)
ISSN 1678-457X (Online)

DOI: https://doi.org/10.1590/fst.45222

Total flavonoids from *Lagerstroemia speciosa* (L.) Pers inhibits TNF-α-induced insulin resistance and inflammatory response in 3T3-L1 adipocytes *via* MAPK and NF-κB signaling pathways

Haowen YIN[1#], Xiaojun YANG[1#], Shaobin LIU[1], Jian ZENG[1], Shaohong CHEN[1], Shilin ZHANG[1], You LIU[1*], Yun-Tao ZHAO[1*]

Abstract

Adipocyte tissue inflammation orchestrates the occurrence and development of diseases induced by obesity. Here, the effects of *Lagerstroemia speciosa* (L.) Pers total flavonoids (LTF) on TNF-α-induced insulin resistance (IR) and inflammatory response in 3T3-L1 adipocytes and underlying mechanisms were studied. Cell glucose uptake test confirmed that TNF-α could induce IR in 3T3-L1 adipocytes. The sensitivity of 3T3-L1 adipocytes to insulin was increased by LTF treatment. The phosphorylation of IRS1 and Akt in TNF-α-treated 3T3-L1 adipocytes was markedly restored by LTF treatment. The results revealed that interleukin-6 (IL-6) and monocyte chemoattractant protein-1 (MCP-1) mRNA expression was elevated in TNF-α-administered 3T3-L1 adipocytes, whereas the mRNA expression of adiponectin (ADPN) was considerably decreased. When treated with 50 μg/mL LTF, the IL-6 and MCP-1 mRNA expression levels were drastically reduced, and the ADPN mRNA expression level was significantly raised. Moreover, the concentration of IL-6 in the supernatant of the medium was decreased after LTF treatment compared with the model group. Western blotting results showed that the phosphorylation of p38, JNK, and ERK of mitogen-activated protein kinase (MAPK) signaling pathways and IκB of NF-κB signaling pathway were inhibited. It suggested that LTF improves TNF-α-induced IR and inflammatory response in 3T3-L1 adipocytes *via* inhibiting MAPK and NF-κB signaling pathways.

Keywords: *Lagerstroemia speciosa* (L.) Pers; 3T3-L1 adipocytes; insulin resistance; inflammatory response.

Practical Application: It not only improves the utilization value of *Lagerstroemia speciosa* (L.) Pers, but also provides a theoretical reference for adding *Lagerstroemia speciosa* (L.) Pers as a base material for nutraceuticals.

1 Introduction

Over the last few decades, obesity has become a global epidemic as a serious public health problem in developed countries and affects developing countries. The incidence of type 2 diabetes (T2D), cardiovascular diseases, hypertension, cancer, and other diseases increases significantly with the prevalence of obesity (Bai et al., 2021; Habibi et al., 2017; Verdeguer et al., 2016). Accumulating data proves that obesity has closely associated with chronic low-grade inflammation, contributing to these diseases. In recent years, adipose tissue has become more than just an energy storage tissue (Jin et al., 2011). More and more studies have proved that adipose tissue, as a vital endocrine organ, can secrete a variety of proteins called adipokines, including resistin, adiponectin (ADPN), leptin, tumor necrosis factor-α (TNF-α), interleukin-6 (IL-6), monocyte chemoattractant protein-1 (MCP-1), intercellular adhesion molecule (ICAM), *etc* (Fried et al., 1998). Researchers confirmed that adipokines could potentially impact adipose tissue inflammation and immune response (van Dierendonck et al., 2020). The reduced sensitivity of the organism to the regular action of insulin is called insulin resistance (IR), and IR performs a key position in the development of T2D. Inflammation is an essential factor in the production of IR. Inflammatory factors can evoke IR by interfering with the insulin signaling transduction pathway (Li et al., 2022; Lontchi-Yimagou et al., 2013). Adipokines can also directly damage pancreatic islet β-cells, leading to T2D (Yaribeygi et al., 2019). Accordingly, it is crucial to explore a drug with significant improvement of IR, anti-inflammatory effects, and a few side effects to prevent and treat obesity-related diseases.

Lagerstroemia speciosa (L.) Pers, also known as Crape Myrtle, a kind of food-medicine dual plant mainly distributed in Southeast Asia, has been used for thousands of years to prevent and treat obesity and T2D (Singh & Ezhilarasan, 2020). In addition, the leaves, flowers, and fruits of *Lagerstroemia speciosa* (L.) Pers are often processed into health drinks. The previous studies have confirmed that the *Lagerstroemia speciosa* (L.) Pers leaves have multi-pharmacological effects such as hypoglycemia, antiobesity, antioxidant, anti-tumor, *etc.*, without toxic and side effects (Judy et al., 2003; Khan et al., 2002; Saumya & Basha, 2011; Suzuki et al., 1999). The main ingredients of *Lagerstroemia*

Received 27 Apr., 2022
Accepted 31 May, 2022
[1] *Guangdong Province Engineering Laboratory for Marine Biological Products, Guangdong Provincial Key Laboratory of Aquatic Product Processing and Safety, Modern Biochemistry Experimental Center, College of Food Science and Technology, Guangdong Ocean University, Zhanjiang, P. R. China*
*Corresponding author: zhaoyt@gdou.edu.cn; liuy6254282@gdou.edu.cn
[#] *These authors contributed equally to this work*

speciosa (L.) Pers leaves that have the effect of hypoglycemia are triterpenoids such as 2α-hydroxy-oleanolic, 2α-hydroxy-ursolic acid, corosolic acid, and maslinic acid, among which corosolic acid is called plant insulin (Miyaji et al., 1999).

To date, the effect of *Lagerstroemia speciosa* (L.) Pers total flavonoids (LTF) on TNF-α-induced IR and inflammatory response in 3T3-L1 adipocytes have not been reported. In this research, we explored LTF inhibits TNF-α-induced IR and inflammatory response in 3T3-L1 adipocytes. Meanwhile, mechanisms underlying the effect of LTF on IR and inflammatory response in 3T3-L1 adipocytes.

2 Materials and methods

2.1 Materials

Fresh samples of *Lagerstroemia speciosa* (L.) Pers were collected from Guangdong Ocean University. Plant authentication was implemented by Prof. Hai Liu, Guangdong Ocean University. 3T3-L1 preadipocytes were bought from Shanghai Institutes for Biological Sciences (Shanghai, China). The TNF-α was obtained from PeproTech Inc. (Cranbury, USA). The fetal bovine serum (FBS) was bought from Hyclone (Logan, USA). The Dulbecco's Modified Eagle Medium (DMEM) was obtained from Gibco (Grand Island, USA). The MTT was purchased from Dingguo Changsheng Biotechnology Co., Ltd (Beijing, China). The M-MLV was purchased from Progema (Madison, USA). The dNTP mixture, oligo d (T) primers, and RNase inhibitor were obtained from Takara (Kusatsu, Japan). The IL-6 ELISA kit was obtained from Thermo (Waltham, USA). The anti-phosphorylated p38, anti-phosphorylated SAPK/JNK, anti-phosphorylated ERK1/2, anti-phosphorylated IκB, and anti-phosphorylated Akt (Ser473) antibodies were purchased from Cell Signaling Technology (Danvers, USA). The anti-phosphorylated IRS1 (Ser307) antibody was purchased from Millipore (Billerica, USA).

2.2 Identification of LTF compounds by UPLC-Triple-TOF-MS/MS

According to the previous protocol (Liu et al., 2013), pulverized sample (10 mg) was reconstituted with 1mL 70% (v/v) ethanol and sonicated for 20 min. The mixture was centrifuged at 10000 g for 15 min to remove precipitation. The supernatant was passed through a 0.22 mm ultrafiltration membrane and awaited analysis.

The sample was analyzed by Acquity™ UPLC (Waters, Milford, USA) and Triple-TOF/MS™ 5600System-MS/MS equipped with an electrospray ionization source. ZORBAX SB-C18 100 mm × 4.6 mm, 1.8 μm chromatographic columns (Agilent, Santa Clara, USA) was used for analysis. The gradient solutions were composed of mobile phase A (0.1% formic acid, v/v) and mobile phase B (0.1% formic acid/acetonitrile, v/v). With a flow rate was 0.8 mL/min and 30 °C column temperature, 95% mobile phase A was initially run for 2 min, 50% mobile phase A was flowed for 23 min, 5% mobile phase A was run for 12 min, and then the final condition of a mixture of 95% mobile phase A and 5% mobile phase B was flowed for 3 min. The following execution parameters were applied: Scan range (m/z 100-1500), nebulizing gas (50 psi), heating gas (50 psi), curtain gas™ (35 psi), heating temperature (550 °C), and spray voltage (4500 V). The Peakview software 2.1 was used to normalize the ionic intensity of each peak relative to the sum of the peak intensities in the sample. Then, The SIMCA-P software was used to analyze normalized data (Peng et al., 2020).

2.3 Cell culture and treatment

According to the previous protocols with some modifications (Huang et al., 2013; Ke et al., 2017). 3T3-L1 preadipocytes were maintained in DMEM containing 1% antibiotic-antimycotic and 10% (v/v) fetal bovine serum (FBS) with a humidified atmosphere containing 5% CO2 at 37 °C. The maintenance medium was altered once for 2 days. After cell contact inhibition, the medium was replaced to DMEM involving 5 μg/mL insulin, 10% (v/v) FBS, 0.5 mM 3-isobutyl-methyl-xanthine, and 0.25 μM dexamethasone. After 2 days, the medium was altered to DMEM, including 10% (v/v) FBS and 5 μg/mL insulin, and stayed for 2 days. The medium was altered with a normal culture medium again and incubated for 4-6 days until more than 90% of cells expressed an adipocyte phenotype.

2.4 Cell viability assay

3T3-L1 adipocytes were seeded into 96-well culture plates at a density of 5×10^4 cells/mL and stayed for 24 h. The cells were divided randomly into four groups: control group (C), low-dose LTF group (L, 0.5 μg/mL), middle-dose LTF group (M, 5 μg/mL), and high-dose LTF group (H, 50 μg/mL), respectively. The cells were cultured with different doses of LTF for 12 h. Then, the cells were washed 3 times with PBS, and 100 μL MTT (0.5 mg/mL) was added to each well for 2 h. The medium was removed, and 150 μL dimethyl sulfoxide was brought to each well and then shaken for 5 min. Absorbance was measured using a TriStar LB941 microplate reader (Berthold, Stuttgart, Germany) at 490 nm. Cell viability assay was performed according to the earlier methods, with suitable modifications (Truong et al., 2019).

2.5 Determination of adipocyte glucose uptake

3T3-L1 adipocytes were divided randomly into three groups: the control group, the model group (T), and the LTF group, respectively. Each group was added with DEME medium, and the medium of the IR and LTF groups contained TNF-α at a concentration of 10 mg/mL. After culturing for 24 h, each group was changed with medium, and the medium of the LTF group contained 50 mg/mL LTF. After continuing the culture for 12 h, the three groups were selected randomly for three bottles and added 10 nM insulin for 30 min of stimulation. The content of glucose was detected by the glucose oxidase-peroxidase method in the cell supernatant. All operations of the glucose determination kit comply with the guidelines.

2.6 qRT-PCR assay

According to the former studies, the qRT-PCR assay was performed with proper modifications (Tian et al., 2022). The total RNA of 3T3-L1 adipocytes was extracted by Trizol reagent (Invitrogen, Carlsbad, USA) following the manufacturer's

protocols. The concentration and purity of obtained RNA were appraised by spectrophotometer and agarose gel electrophoresis, respectively. According to the product instructions, M-MLV, dNTP mixture, oligo d $(T)_{18}$ primer, and RNase inhibitor were configured with a reaction system to synthesize cDNA. The SYBR Premix Ex Taq II kit (Takara, Kusatsu, Japan) was applied to qRT-PCR. The cycle conditions are as follows: 94 °C for 40 s; 45 cycles of 94 °C for 5 s; several annealing temperatures for 15 s, and 72 °C for 15 s. The PCR primers were as follows: β-actin forward, 5'-TTCGTTGCCGGTCCACA-3' and reverse, 5'-ACCAGCGCAGCGATATCG-3'; MCP-1 forward, 5'-TTCCTCCACCACCATGCAG-3' and reverse, 5'- CCAGCCGGCAACTGTGA-3'; IL-6 forward, 5'- AACGATGATGCACTTGCAGA-3' and reverse, 5'-GAGCATTGGAAATTGGGGTA-3'; ADPN forward, 5'-GGAGAGAAAGGAGATGCAGGT-3' and reverse, 5'-CTTTCCTGCCAGGGGTTC-3'. The melts curve analysis was conducted to verify amplification specificity, and the relative mRNA expression levels were analyzed using the $2^{-\Delta\Delta Ct}$ method with β-actin as an endogenous reference.

2.7 ELISA assay for IL-6 release

In order to further verify the inhibitory effect of LTF on inflammatory response in 3T3-L1 adipocytes, the supernatant of the culture medium was centrifugated. According to operating instructions, the medium of 3 h, 6 h, and 12 h was evaluated for IL-6 released using ELISA kits.

2.8 Western blotting analysis

3T3-L1 adipocytes were lysed in 250 μL of radioimmunoprecipitation assay (RIPA) buffer containing protease and phosphatase inhibitors (Zhao et al., 2022). The lysate was centrifuged at 11000 g for 12 min, and then the supernatant was collected. The protein concentration was tested *via* the BCA assay kit. The Western blotting analysis was followed the previous report with specific changes (Xiao et al., 2020). The 12% sodium dodecyl sulfate-polyacrylamide gel electrophoresis (SDS-PAGE) and polyvinylidene fluoride (PVDF) membrane were used to separate samples. The membrane was blocked in 5% bovine serum albumin for 2 h. Hereafter, the membrane was incubated with the primary antibodies for 12 h, and the secondary antibody conjugated with horseradish peroxidase for 2 h. TBST was applied to the membrane for thorough cleaning. ECL kit was used on the membrane, and the Western blotting was photographed *via* the ChemiDoc™ XRS + System (Bio-Rad, Hercules, USA). The intensity of the protein bands was normalized to β-actin.

2.9 Statistical analysis

All experimental data were expressed as mean ± standard deviation (SD). Statistical comparison was carried out using one-way analysis of variance (ANOVA) followed by Turkey's multiple analysis using the GraphPad Prism 8.0. The values of $P < 0.05$ were considered statistically significant.

3 Results

3.1 Identification and relative content comparison of LTF

The total ion current chromatogram of the sample showed a powerful signal, superior retention, and large peak capacity (Figure 1). A total of 6 flavonoids were identified, including quercetin-3'-sulfate, ellagic acid, 3'-O-methylellagic acid-4-O-β-D-glucoside, 3'-O-methyl-4-O-β-D-xylopyranosyl ellagic acid, 3'-O-methyl-4-O-β-D-xylopyranosyl ellagic acid, 3-O-methylellagic acid 4'-sulfate, and kaempferol 3-monosulphate (Figure 2). The Triple-TOF mass spectrometer figures of the 6 *Lagerstroemia speciosa* (L.) Pers flavonoids were supplied in Supplementary data.

3.2 Effect of LTF on 3T3-L1 cell viability

The cytotoxic effects of LTF on 3T3-L1 cell viability were evaluated by MTT assay. The viabilities of cells treated with LTF (0.5, 5.0, and 50.0 μg/mL, respectively) showed no cytotoxicity at 12 h (Figure 3). To investigate the possible mechanisms of LTF inhibits IR and inflammatory responses, 3T3-L1 adipocytes exposed to TNF-α and treated with a 50.0 μg/mL dose of LTF were selected for in-depth study.

3.3 Effect of LTF on IR

The glucose content in the medium of 3T3-L1 adipocytes after exposure to LTF for 12 h was calculated to explore the effect of LTF on glucose consumption. The glucose consumption of the control group was seen as 1, and the other groups were compared with it. After the cells in each group were stimulated by insulin,

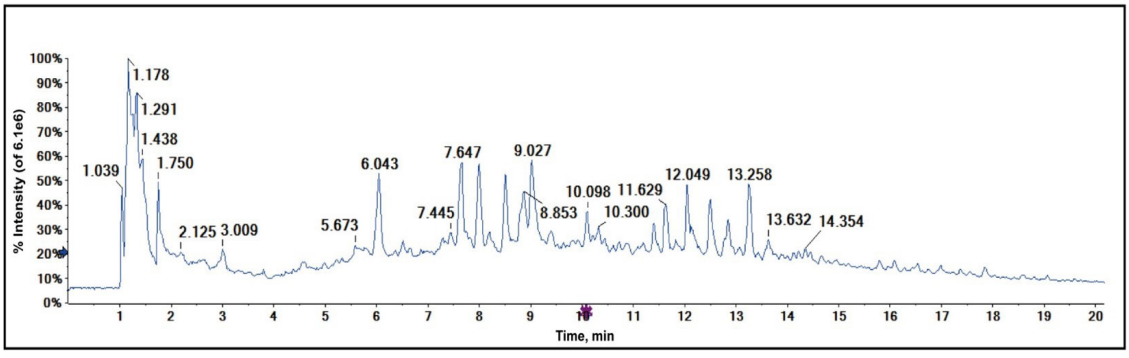

Figure 1. Total ion current chromatogram of the LTF in electron spray ionization (ESI)-mode.

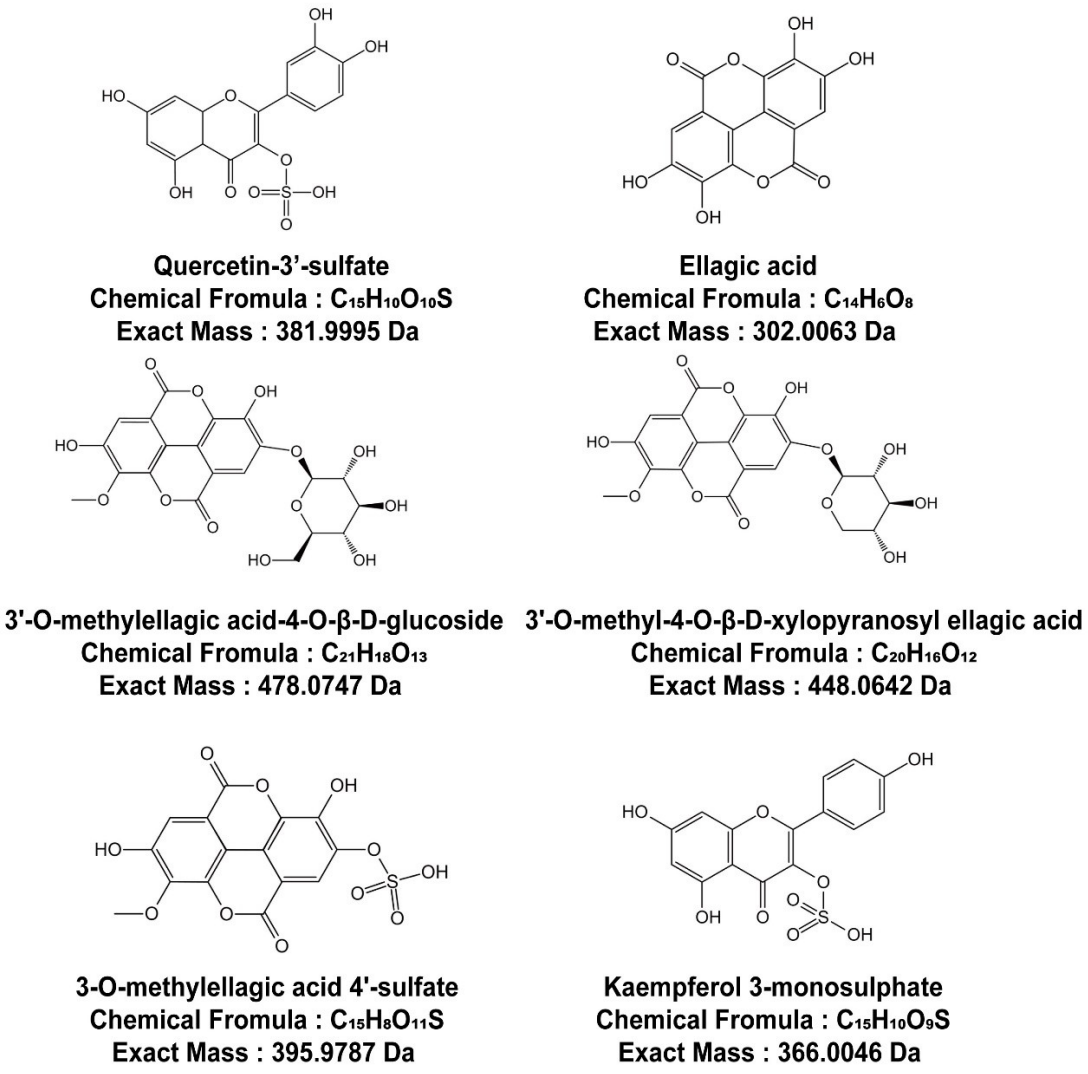

Figure 2. Structure of identified LTF.

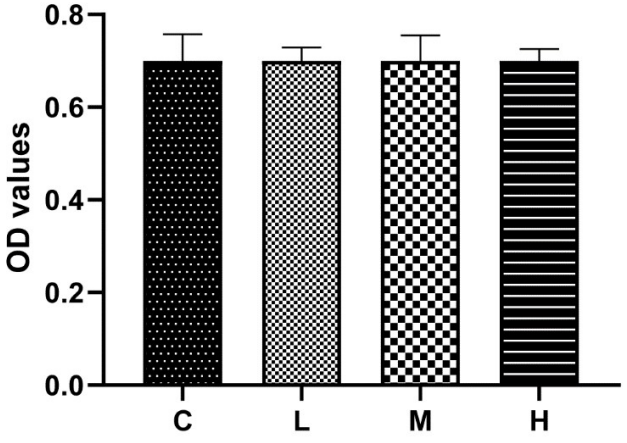

Figure 3. The results of the cell viability experiment. All data were shown as the mean ± SD (n = 3). C group: the control group. L group: the low-dose LTF group (0.5 μg/mL). M group: the middle-dose LTF group (5 μg/mL). H group: the high-dose LTF group (50 μg/mL).

the glucose uptake was increased. The glucose uptake of the TNF-α-treated cells was lower than that of the control group, with or without insulin stimulation, indicating that the cells were less sensitive to insulin and appeared to the phenomenon of insulin resistance. LTF-administered cells could significantly increase the insulin sensitivity of 3T3-L1 adipocytes to alleviate insulin resistance ($P < 0.01$, Figure 4A). Therefore, we considered the effect of LTF on insulin transmembrane signaling. The expression stages of the phosphorylation of Akt and IRS1 signaling pathways were investigated by Western blotting (Figure 4B-4C). The Akt phosphorylation was dramatically inhibited by TNF-α in 3T3-L1 adipocytes, which was dramatically improved by LTF ($P < 0.01$, Figure 4D). Moreover, the significant inhibition effect of the LTF on IRS1 (Ser307) phosphorylation in 3T3-L1 adipocytes was observed ($P < 0.01$, Figure 4E), which had insulin resistance induced by TNF-α. It can be inferred that the improvement effect of LTF on insulin resistance of the adipocytes is mainly due to inhibition of Ser 307 phosphorylation of IRS1 and promotion of Akt phosphorylation, the downstream effector of the insulin signaling pathway.

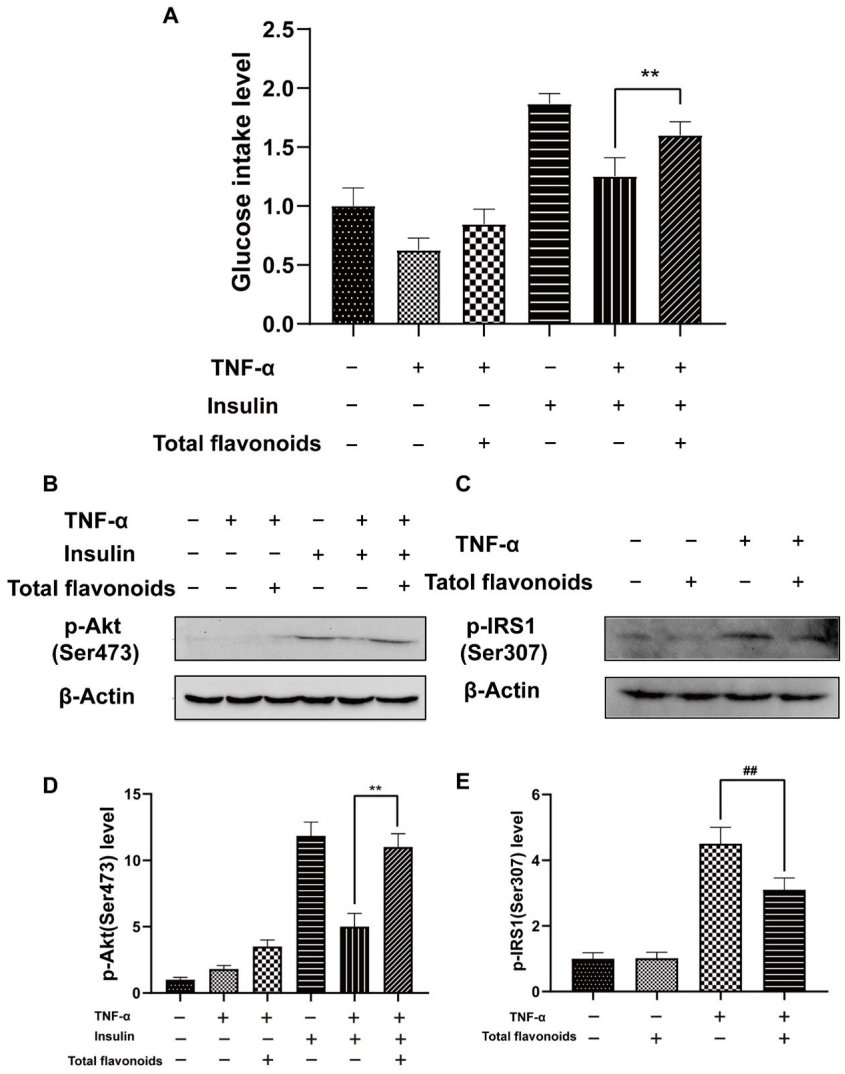

Figure 4. The effects of LTF on IR. (A) The effects of LTF on cell glucose uptake. (B, C) Representative image of Western blotting results. (D, E) Quantification of the protein expression of p-Akt (Ser473) and p-IRS1 (Ser307). All data were shown as the mean ± SD (n = 3). $^{**}P < 0.01$, $^{\#\#}P < 0.01$.

3.4 Effect of LTF on adipokines expression

Compared with that in the control group, the relative expression levels of IL-6 and MCP-1 mRNA in the model group cells at each time point were dramatically increased ($P < 0.01$, Figure 5A-5B). The result indicated that 3T3-L1 adipocytes induced inflammation after TNF-α induction, and the inflammation model was successfully constructed. The IL-6 mRNA expression level of the cells was markedly lower than that of the model group ($P < 0.05$, Figure 5A-5B). The expression level of MCP-1 mRNA in each group of cells was dramatically decreased ($P < 0.05$, $P < 0.01$, Figure 5A-5B) compared to the model group. Compared with that of the model group, the ADPN mRNA expression level of the high-dose LTF group was obviously reduced ($P < 0.05$, $P < 0.01$, Figure 5C), showing a significant dose-effect relationship. In order to further verify the inhibitory effect of LTF on the inflammatory response of 3T3-L1 adipocytes, IL-6 in the culture medium was tested. The cells were administered with LTF for 12 h and 24 h, respectively. Compared with the control group, IL-6 in the medium of the model group was significantly increased ($P < 0.05$, Figure 5D), and the high-dose LTF group reversed this situation most obviously ($P < 0.01$, Figure 5D).

3.5 Effect of LTF on MAPK and NF-κB signaling pathways

We considered the viable mechanisms concerned with the effects of LTF on TNF-α-induced inflammatory response. The expression stages of the mitogen-activated protein kinase (MAPK) and NF-κB signaling pathways were investigated by Western blotting (Figure 6). The p38, JNK, and ERK of 3T3-L1 adipocytes were phosphorylated by TNF-α, which was markedly inhibited by LTF($P < 0.05$, $P < 0.01$, Figure 6). The results showed that LTF might have anti-inflammatory activity by inhibiting the phosphorylation level of the MAPK pathway. IκB, the essential protein of the NF-κB signaling pathway, was phosphorylated under the action of TNF-α, and phosphorylation was inhibited after adding LTF at a final concentration of 50 ug/mL. Among

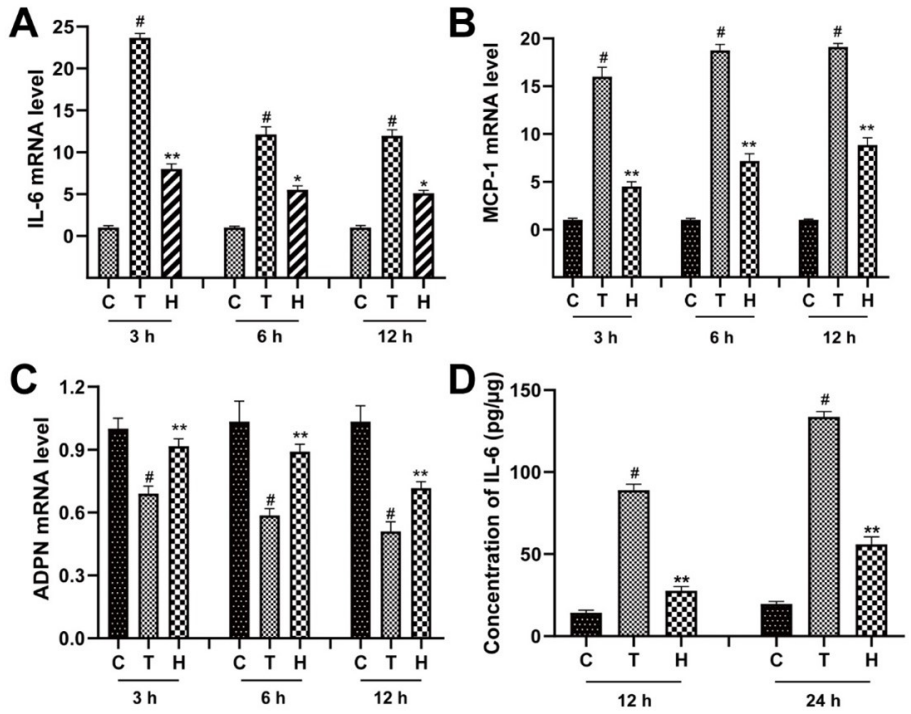

Figure 5. The effects of LTF on mRNA expression of adipokines changes. (A, B, and C) Quantification of the mRNA expression of IL-6, MCP-1, and ADPN. (D) The effects of LTF on IL-6 release. C group: the control group. T group: the model group. H group: the high-dose LTF group (50 μg/mL). All data were shown as the mean ± SD (n = 3). #P < 0.05 compared with that of the control group, *P < 0.05, **P < 0.01 compared with that of the model group.

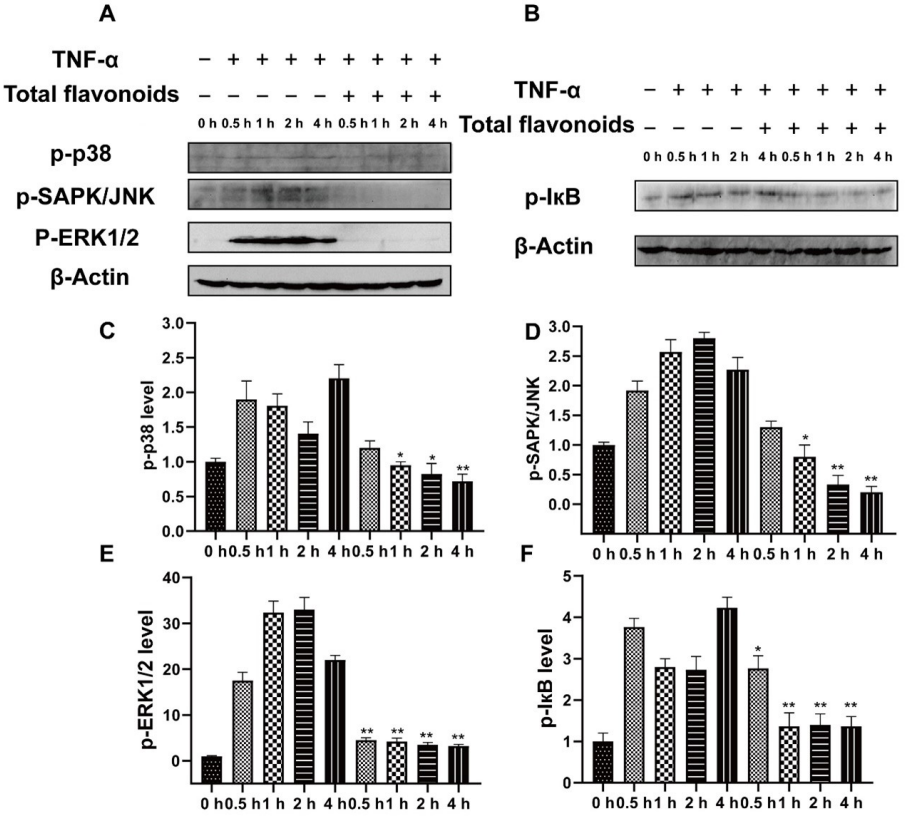

Figure 6. The effects of LTF on MAPK and NF-κB signaling pathways. (A, B) Representative image of Western blotting results. (C, D, E, and F) Quantification of the protein expression of p-p38, p-SAPK/JNK, p-ERK1/2, and p-IκB. All data were shown as the mean ± SD (n = 3). *P < 0.05, **P < 0.01 compared with that of the TNF-α group.

them, the inhibitory effect of 1, 2, and 4 h was significant ($P < 0.01$, Figure 6B and 6F) compared to the TNF-α group.

4 Discussion

Obesity is one of the risk factors for cardiovascular disease, which can cause chronic low-grade inflammation in adipose tissue (You et al., 2022). Accumulating literature shows that obesity can contribute to IR and T2D. In this study, the total flavonoids in *Lagerstroemia speciosa* (L.) Pers were extracted by ethanol, and a total of 6 flavonoids were identified. The effect of LTF on TNF-α induced IR, and inflammatory response in 3T3-L1 adipocytes was investigated. We found that LTF can alleviate IR and inflammatory response in 3T3-L1 adipocytes induced by TNF-α. In this research, the mechanisms underlying the impact of LTF on TNF-α induced IR and inflammatory response in 3T3-L1 adipocytes were studied.

3T3-L1 adipocytes are studied adipocytes metabolism and differentiation as a mature cell model, specifically induced to differentiate into mature adipocytes by 3-isobutyl-1-methylxanthine (IBMX), dexamethasone, and insulin (Poulos et al., 2010). So as to determine the degree of toxicity of LTF towards 3T3-L1 adipocytes, the different doses of LTF were added to the medium to observe its effect on cell growth, morphology, and differentiation. In parallel, the MTT staining method was used to determine the effect of LTF on the survival rate of 3T3-L1 adipocytes. Our results show that the three doses of LTF had no significant effect on cell proliferation and cell survival, which confirmed that it is appropriate to use 3T3-L1 adipocytes for follow-up experimental research.

Obesity-induced chronic low-grade inflammation is an essential factor leading to insulin resistance in the organism. TNF-α can induce IR in 3T3-L1 adipocytes as an inflammatory factor (Anusree et al., 2018). Cell glucose uptake test confirmed that TNF-α could induce IR in 3T3-L1 adipocytes, and LTF could increase the sensitivity of 3T3-L1 adipocytes to insulin, thereby promoting glucose uptake by 3T3-L1 adipocytes. IRS1 is a crucial component of insulin signaling, which is tyrosine phosphorylated in response to insulin to activate the phosphorylation of PI3K/Akt. PI3K/Akt reflects this signal to the body, thereby completing the transmembrane transmission of signals (Kim et al., 2018; Pal et al., 2019; Rubio-Ruiz et al., 2019). Here, we observed that phosphorylation of Ser307 in the IRS competitively inhibits tyrosine phosphorylation, with consequently diminished binding to the insulin receptor. LTF could inhibit Ser 307 phosphorylation of IRS1 and promote Akt phosphorylation, the downstream effector of the insulin signaling pathway.

Inflammation is an essential factor in the production of IR. IL-6 is an essential inflammatory factor involved in immune regulation and inflammatory response (Chen et al., 2015). The data have exhibited that the expression of IL-6 in serum is positively correlated with the degree of the inflammatory response (Stamatakis et al., 2008). MCP-1 acts as a potent chemoattractant and activator of monocytes/macrophages, which plays a role in chronic inflammation (Ohtaki et al., 2012). ADPN is a cytokine secreted by white adipose tissue, increasing the body's sensitivity to insulin, thereby alleviating the insulin resistance (Khoramipour et al., 2021). According to reports, ADPN could also inhibit the production and release of TNF-α and has a particular anti-inflammatory effect (Rebollo-Hernanz et al., 2019). Thence, the IL-6, MCP-1, and ADPN mRNA expression levels were detected. We observed that the IL-6 and MCP-1 mRNA expression levels were significantly elevated with LTF treatment, whereas the expression of ADPN mRNA was observably decreased. Therefore, LTF could alleviate the cellular inflammatory response caused by TNF-α in 3T3-L1 adipocytes.

MAPK is one of the vital signal transduction systems in organisms, and it participates in mediating various cellular processes such as growth, development, division, differentiation, death, and intercellular functional synchronization (Yang et al., 2017; Zhao et al., 2019). The threonine and tyrosine on the T-loop structure of the three subfamilies of MAPK (p38, JNK, ERK) are activated by dual phosphorylation under the stimulation of TNF-α (Foletta et al., 1998; Shin et al., 2021). Then, the MAPK subfamily undergoes nuclear enters the nucleus to link the inflammatory response element on DNA, upregulating the expression of downstream inflammation genes (such as TNF-α, IL-1, IL-6, and other adipokines) (Ono & Han, 2000). TNF-α can activate IKK, phosphorylate IκB, and dissociate from NF-κB, thereby intensifying the inflammatory response caused by insulin resistance (Li et al., 2018; Li et al., 2015). Here, we found that the phosphorylation of MAPK and NF-κB signaling pathways were dramatically inhibited after LTF treatment.

5 Conclusion

In summary, this study demonstrates that LTF effectively ameliorates TNF-α-induced IR and inflammatory response in 3T3-L1 adipocytes *via* regulating the MAPK and NF-κB signaling pathways. LTF might be applied as a novel candidate to develop functional foods.

Conflict of interest

The authors declare no conflict of interest.

Author contributions

Conceptualization: Yun-Tao Zhao. Data curation: Haowen Yin, Xiaojun Yang, Shaobin Liu, and Jian Zeng. Investigation: Haowen Yin, Shaobin Liu, Shaohong Chen, Shilin Zhang. Resources: Yun-Tao Zhao, You Liu. Writing-original draft: Shaobin Liu.

Acknowledgements

The present study was supported by the grants of the Natural Science Foundation of Guangdong Ocean University (C08126), the Innovation and Entrepreneurship Training Program for College Students (201810566006), and the Innovative Team Program of High Education of Guangdong Province (2021KCXTD021).

References

Anusree, S. S., Sindhu, G., Rani, M. R. P., & Raghu, K. G. (2018). Insulin resistance in 3T3-L1 adipocytes by TNF-α is improved by

punicic acid through upregulation of insulin signaling pathway and endocrine function, and downregulation of proinflammatory cytokines. *Biochimie*, 146, 79-86. http://dx.doi.org/10.1016/j.biochi.2017.11.014. PMid:29180021.

Bai, Q., Xu, J., Zhu, W., Huang, C., Ni, X., Zhao, H., Feng, X., Li, L., Du, S., Fan, R., & Wang, J. (2021). Effects of consumption of a low glycaemic index formula on glycaemic control in patients with type 2 diabetes managed by medical nutrition therapy. *Food Science and Technology*, 41(3), 768-774. http://dx.doi.org/10.1590/fst.51320.

Chen, Y., Wu, B., Liu, L., You, X., Chen, L., Wu, Y., & Zhang, Q. (2015). Recombinant Cpn 0810 stimulates proinflammatory cytokine expression and apoptosis in human monocytes. *Experimental and Therapeutic Medicine*, 9(2), 459-463. http://dx.doi.org/10.3892/etm.2014.2111. PMid:25574216.

Foletta, V. C., Segal, D. H., & Cohen, D. R. (1998). Transcriptional regulation in the immune system: all roads lead to AP-1. *Journal of Leukocyte Biology*, 63(2), 139-152. http://dx.doi.org/10.1002/jlb.63.2.139. PMid:9468273.

Fried, S. K., Bunkin, D. A., & Greenberg, A. S. (1998). Omental and subcutaneous adipose tissues of obese subjects release interleukin-6: depot difference and regulation by glucocorticoid. *The Journal of Clinical Endocrinology and Metabolism*, 83(3), 847-850. http://dx.doi.org/10.1210/jc.83.3.847. PMid:9506738.

Habibi, J., Aroor, A. R., Sowers, J. R., Jia, G., Hayden, M. R., Garro, M., Barron, B., Mayoux, E., Rector, R. S., Whaley-Connell, A., & DeMarco, V. G. (2017). Sodium glucose transporter 2 (SGLT2) inhibition with empagliflozin improves cardiac diastolic function in a female rodent model of diabetes. *Cardiovascular Diabetology*, 16(1), 9. http://dx.doi.org/10.1186/s12933-016-0489-z. PMid:28086951.

Huang, C. Y., Yao, W. F., Wu, W. G., Lu, Y. L., Wan, H., & Wang, W. (2013). Endogenous CSE/H2 S system mediates TNF-α-induced insulin resistance in 3T3-L1 adipocytes. *Cell Biochemistry and Function*, 31(6), 468-475. http://dx.doi.org/10.1002/cbf.2920. PMid:23080424.

Jin, L., Shi, G., Ning, G., Li, X., & Zhang, Z. (2011). Andrographolide attenuates tumor necrosis factor-alpha-induced insulin resistance in 3T3-L1 adipocytes. *Molecular and Cellular Endocrinology*, 332(1-2), 134-139. http://dx.doi.org/10.1016/j.mce.2010.10.005. PMid:20943205.

Judy, W. V., Hari, S. P., Stogsdill, W. W., Judy, J. S., Naguib, Y. M., & Passwater, R. (2003). Antidiabetic activity of a standardized extract (Glucosol™) from *Lagerstroemia speciosa* leaves in type II diabetics. a dose-dependence study. *Journal of Ethnopharmacology*, 87(1), 115-117. http://dx.doi.org/10.1016/S0378-8741(03)00122-3. PMid:12787964.

Ke, B., Ke, X., Wan, X., Yang, Y., Huang, Y., Qin, J., Hu, C., & Shi, L. (2017). Astragalus polysaccharides attenuates TNF-α-induced insulin resistance *via* suppression of miR-721 and activation of PPAR-γ and PI3K/AKT in 3T3-L1 adipocytes. *American Journal of Translational Research*, 9(5), 2195-2206. PMid:28559971.

Khan, M. T., Lampronti, I., Martello, D., Bianchi, N., Jabbar, S., Choudhuri, M. S., Datta, B. K., & Gambari, R. (2002). Identification of pyrogallol as an antiproliferative compound present in extracts from the medicinal plant Emblica officinalis: effects on in vitro cell growth of human tumor cell lines. *International Journal of Oncology*, 21(1), 187-192. http://dx.doi.org/10.3892/ijo.21.1.187. PMid:12063567.

Khoramipour, K., Chamari, K., Hekmatikar, A. A., Ziyaiyan, A., Taherkhani, S., Elguindy, N. M., & Bragazzi, N. L. (2021). Adiponectin: structure, physiological functions, role in diseases, and effects of nutrition. *Nutrients*, 13(4), 1180. http://dx.doi.org/10.3390/nu13041180. PMid:33918360.

Kim, E., Kim, D. H., Singaram, I., Jeong, H., Koh, A., Lee, J., Cho, W., & Ryu, S. H. (2018). Cellular phosphatase activity of C1-Ten/Tensin2 is controlled by Phosphatidylinositol-3,4,5-triphosphate binding through the C1-Ten/Tensin2 SH2 domain. *Cellular Signalling*, 51, 130-138. http://dx.doi.org/10.1016/j.cellsig.2018.07.009. PMid:30092354.

Li, A., Shen, P., Liu, S., Wang, J., Zeng, J., & Du, C. (2022). Vitamin D alleviates skeletal muscle loss and insulin resistance by inducing vitamin D receptor expression and regulating the AMPK/SIRT1 signaling pathway in mice. *Food Science and Technology*, 42, e47921. http://dx.doi.org/10.1590/fst.47921.

Li, J., Xue, Y. M., Zhu, B., Pan, Y. H., Zhang, Y., Wang, C., & Li, Y. (2018). Rosiglitazone elicits an adiponectin-mediated insulin-sensitizing action at the adipose tissue-liver axis in Otsuka Long-Evans Tokushima Fatty Rats. *Journal of Diabetes Research*, 2018, 4627842. http://dx.doi.org/10.1155/2018/4627842. PMid:30225267.

Li, M., Han, Z., Bei, W., Rong, X., Guo, J., & Hu, X. (2015). Oleanolic acid attenuates insulin resistance *via* NF-κB to regulate the IRS1-GLUT4 pathway in HepG2 cells. *Evidence-Based Complementary and Alternative Medicine*, 2015, 643102. http://dx.doi.org/10.1155/2015/643102. PMid:26843885.

Liu, S.-B., Chen, S., Zhao, Y.-T., & Liu, Y. (2013). Study on the extractive technology of total flavonoids in Lagerstroemia speciosa leaf. *Anhui Nongye Kexue*, 41(3), 970-972.

Lontchi-Yimagou, E., Sobngwi, E., Matsha, T. E., & Kengne, A. P. (2013). Diabetes mellitus and inflammation. *Current Diabetes Reports*, 13(3), 435-444. http://dx.doi.org/10.1007/s11892-013-0375-y. PMid:23494755.

Miyaji, N., Kazama, M., Ina, H., Yamada, K., & Yamakawa, T. (1999). Influence of Banaba-Kuwa extracted powder on plasma glucose level in rat. *Journal of Translational Medicine*, 16, 208-211.

Ohtaki, H., Ito, H., Hoshi, M., Osawa, Y., Takamatsu, M., Hara, A., Ishikawa, T., Moriwaki, H., Saito, K., & Seishima, M. (2012). High susceptibility to lipopolysaccharide-induced lethal shock in encephalomyocarditis virus-infected mice. *Scientific Reports*, 2(1), 367. http://dx.doi.org/10.1038/srep00367. PMid:22509465.

Ono, K., & Han, J. (2000). The p38 signal transduction pathway: activation and function. *Cellular Signalling*, 12(1), 1-13. http://dx.doi.org/10.1016/S0898-6568(99)00071-6. PMid:10676842.

Pal, M., Khan, J., Kumar, R., Surolia, A., & Gupta, S. (2019). Testosterone supplementation improves insulin responsiveness in HFD fed male T2DM mice and potentiates insulin signaling in the skeletal muscle and C2C12 myocyte cell line. *PLoS One*, 14(11), e0224162. http://dx.doi.org/10.1371/journal.pone.0224162. PMid:31693697.

Peng, X., Luo, Y., Wang, J., Ji, T., Yuan, L., & Kai, G. (2020). Integrated analysis of the transcriptome, metabolome and analgesic effect provide insight into potential applications of different parts of Lindera aggregata. *Food Research International*, 138(Pt B), 109799. http://dx.doi.org/10.1016/j.foodres.2020.109799. PMid:33288181.

Poulos, S. P., Dodson, M. V., & Hausman, G. J. (2010). Cell line models for differentiation: preadipocytes and adipocytes. *Experimental Biology and Medicine*, 235(10), 1185-1193. http://dx.doi.org/10.1258/ebm.2010.010063. PMid:20864461.

Rebollo-Hernanz, M., Zhang, Q., Aguilera, Y., Martín-Cabrejas, M. A., & Mejia, E. G. (2019). Relationship of the phytochemicals from coffee and cocoa by-products with their potential to modulate biomarkers of metabolic syndrome in vitro. *Antioxidants*, 8(8), 279. http://dx.doi.org/10.3390/antiox8080279. PMid:31387271.

Rubio-Ruiz, M. E., Guarner-Lans, V., Cano-Martínez, A., Díaz-Díaz, E., Manzano-Pech, L., Gamas-Magaña, A., Castrejón-Tellez, V., Tapia-Cortina, C., & Pérez-Torres, I. (2019). Resveratrol and quercetin administration improves antioxidant defenses and reduces fatty liver in metabolic syndrome rats. *Molecules*, 24(7), 1297. http://dx.doi.org/10.3390/molecules24071297. PMid:30987086.

Saumya, S. M., & Basha, P. M. (2011). Antioxidant effect of Lagerstroemia speciosa Pers (banaba) leaf extract in streptozotocin-induced diabetic mice. *Indian Journal of Experimental Biology*, 49(2), 125-131. PMid:21428214.

Shin, K. S., Seo, H., Lee, S. J., Sung, S., & Hwang, D. (2021). Polysaccharide isolated from Korean-style soy sauce activates macrophages *via* the MAPK and NK-κB pathways. *Food Science and Technology*, 41(4), 817-824. http://dx.doi.org/10.1590/fst.06121.

Singh, T. R., & Ezhilarasan, D. (2020). Ethanolic extract of Lagerstroemia Speciosa (L.) Pers., induces apoptosis and cell cycle arrest in HepG2 cells. *Nutrition and Cancer*, 72(1), 146-156. http://dx.doi.org/10.1080/01635581.2019.1616780. PMid:31149840.

Stamatakis, K., Sanders, M. H., Caffo, B., Resnick, H. E., Gottlieb, D. J., Mehra, R., & Punjabi, N. M. (2008). Fasting glycemia in sleep disordered breathing: lowering the threshold on oxyhemoglobin desaturation. *Sleep*, 31(7), 1018-1024. PMid:18652097.

Suzuki, Y., Unno, T., Ushitani, M., Hayashi, K., & Kakuda, T. (1999). Antiobesity activity of extracts from Lagerstroemia speciosa L. leaves on female KK-Ay mice. *Journal of Nutritional Science and Vitaminology*, 45(6), 791-795. http://dx.doi.org/10.3177/jnsv.45.791. PMid:10737232.

Tian, L., Sun, S., Wang, J., Li, W., & Wang, X. (2022). GINS2 affects activity/differentiation, apoptosis and proliferation of osteoblast and osteoclast in steroid-induced osteonecrosis of the femoral head by regulating P53/GADD45A signaling pathway. *Food Science and Technology*, 42, e09921. http://dx.doi.org/10.1590/fst.09921.

Truong, C. S., Seo, E., & Jun, H. S. (2019). Psoralea corylifolia L. seed extract attenuates Methylglyoxal-induced insulin resistance by inhibition of advanced glycation end product formation. *Oxidative Medicine and Cellular Longevity*, 2019, 4310319. http://dx.doi.org/10.1155/2019/4310319. PMid:31976027.

van Dierendonck, X. A. M. H., Sancerni, T., Alves-Guerra, M.-C., & Stienstra, R. (2020). The role of uncoupling protein 2 in macrophages and its impact on obesity-induced adipose tissue inflammation and insulin resistance. *The Journal of Biological Chemistry*, 295(51), 17535-17548. http://dx.doi.org/10.1074/jbc.RA120.014868. PMid:33453996.

Verdeguer, F., Soustek, M. S., Hatting, M., Blättler, S. M., McDonald, D., Barrow, J. J., & Puigserver, P. (2016). Brown adipose YY1 deficiency activates expression of secreted proteins linked to energy expenditure and prevents diet-induced obesity. *Molecular and Cellular Biology*, 36(1), 184-196. http://dx.doi.org/10.1128/MCB.00722-15. PMid:26503783.

Xiao, Z., Huang, X., Chen, J., Yang, S., Liu, Y., & Qian, Z. (2020). Effect of abalone polypeptide on LPS induced HUVEC cell inflammation. *Journal of Guangdong Ocean University*, 40(06), 108-115.

Yang, L., Liu, J., & Qi, G. (2017). Mechanism of the effect of saikosaponin on atherosclerosis in vitro is based on the MAPK signaling pathway. *Molecular Medicine Reports*, 16(6), 8868-8874. http://dx.doi.org/10.3892/mmr.2017.7691. PMid:28990046.

Yaribeygi, H., Atkin, S. L., Simental-Mendía, L. E., & Sahebkar, A. (2019). Molecular mechanisms by which aerobic exercise induces insulin sensitivity. *Journal of Cellular Physiology*, 234(8), 12385-12392. http://dx.doi.org/10.1002/jcp.28066. PMid:30605232.

You, D., Jung, B. C., Villivalam, S. D., Lim, H.-W., & Kang, S. (2022). JMJD8 is a novel molecular nexus between adipocyte-intrinsic inflammation and insulin resistance. *Diabetes*, 71(1), 43-59. http://dx.doi.org/10.2337/db21-0596.

Zhao, Y.-T., Yin, H., Hu, C., Zeng, J., Shi, X., Chen, S., Zhang, K., Zheng, W., Wu, W., & Liu, S. (2022). Tilapia skin peptides restore cyclophosphamide-induced premature ovarian failure via inhibiting oxidative stress and apoptosis in mice. *Food & Function*, 13(3), 1668-1679. http://dx.doi.org/10.1039/D1FO04239D. PMid:35083997.

Zhao, Z., Liu, K., Tian, X., Sun, M., Wei, N., Zhu, X., Yang, H., Wang, T., Jiang, G., & Chen, K. (2019). Effects of RhoC downregulation on the angiogenesis characteristics of myeloma vascular endothelial cells. *Cancer Medicine*, 8(7), 3502-3510. http://dx.doi.org/10.1002/cam4.2208. PMid:31062507.